

Content from this work may be used under the terms of the CC BY 3.0 licence (© 2019). Any distribution of this work must maintain attribution to the author(s), title of the work, publisher, and DOI

OPERATION AND PERFORMANCE OF THE CERN LARGE HADRON COLLIDER DURING PROTON RUN 2

R. Steerenberg[†], R. Alemany-Fernandez, M. Albert, T. Argyropoulos, E. Bravin, G. Crockford, J.-C. Dumont, K. Fuchsberger, R. Giachino, M. Giovannozzi, G.-H. Hemelsoet, W. Höfle, D. Jacquet, M. Lamont, E. Métral, D. Nisbet, G. Papotti, M. Pojer, L. Ponce, S. Redaelli, B. Salvachua, M. Schaumann, M. Solfaroli Camillocci, R. Suykerbuyk, G. Trad, S. Uznanski, J. Uythoven, D. Walsh, J. Wenninger, M. Zerlauth, CERN, 1211 Geneva 23, Switzerland

Abstract

Run 2 of the CERN Large Hadron Collider (LHC) started in April 2015 and was successfully completed on 10th December 2018, achieving largely all goals set in terms of luminosity production. Following the first two-year long shutdown and the re-commissioning in 2015 at 6.5 TeV, the beam performance was increased to reach a peak luminosity of more than twice the design value and a colliding beam time ratio of 50%. This was accomplished thanks to the increased beam brightness from the injector chain, the high machine availability and the performance enhancements made in the LHC for which some methods and tools, foreseen for the High Luminosity LHC (HL-LHC) were tested and deployed operationally. This contribution provides an overview of the operational aspects, main limitations and achievements for the proton Run 2.

LHC PERFORMANCE SUMMARY

This contribution summarizes the LHC proton operation [1], as such the heavy ion periods during Run 2 [2-6] are not subject of this contribution.

The LHC produced 160 fb⁻¹ of integrated luminosity at a beam energy of 6.5 TeV during Run 2 for each of the two high-luminosity experiments, ATLAS and CMS, resulting in a total of 189 fb⁻¹ accumulated for Run 1 and 2 combined. Figure 1 provides a yearly overview of the integrated luminosity since the start of the LHC. From this plot, the commissioning years 2011 (Run 1) and 2015 (Run 2) can clearly be distinguished from the production years 2012 (Run 1), 2016, 2017 and 2018 (Run 2).

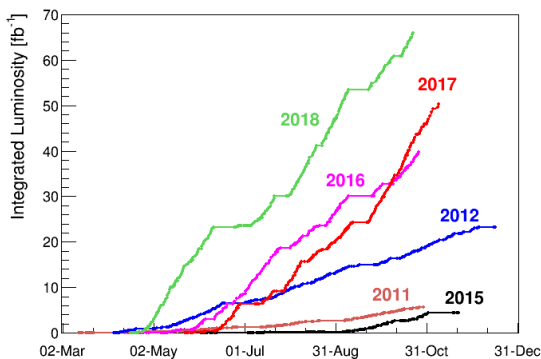


Figure 1: Overview of the integrated LHC luminosity.

The design peak luminosity of $1 \times 10^{34} \text{ cm}^{-2}\text{s}^{-1}$, indicated by the green dotted line in Fig. 2, was exceeded in 2016 and a record peak luminosity of $2.07 \times 10^{34} \text{ cm}^{-2}\text{s}^{-1}$ was

reached in 2018. In 2018, the LHC was routinely operated with an average peak luminosity that was twice the design value, mainly thanks to the higher-than-design beam brightness from the injector chain and the lower-than-design value of the β -function at the interaction points (β^*).

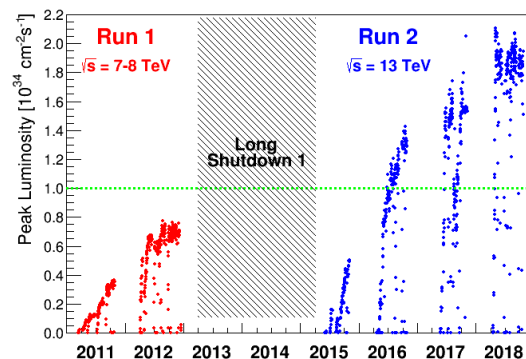


Figure 2: Evolution of the peak luminosity.

Not only the high peak luminosity resulted in a higher integrated luminosity, but also the time the beams were actually in collision, the stable beam time ratio, exceeded initial expectations. Table 1 provides an overview of the LHC availability and its time distribution [7-9]. During the production years, 2016 until 2018, the beams were actually in collision for close to 50% of the scheduled machine time.

Table 1: Machine Availability Breakdown for Protons

| Year | Stable Beam | Downtime | Operation |
|------|--------------|-------------|--------------|
| 2015 | 33% (455 h) | 30% (426 h) | 37% (511 h) |
| 2016 | 49% (1840 h) | 26% (980 h) | 25% (919 h) |
| 2017 | 49% (1634 h) | 19% (653 h) | 32% (1075 h) |
| 2018 | 49% (1932 h) | 24% (943 h) | 27% (1069 h) |

Many of the machine and beam parameters evolved during Run 2 either under the influence of issues encountered or as a result of performance-enhancing changes that were implemented. Table 2 gives an overview of the main parameters for the Run 2 compared to the LHC design values [10].

LHC OPERATION SUMMARY

The LHC started in 2015 at 6.5 TeV with 50 ns bunch spacing to minimize e-cloud effects. The switch to the standard 25 ns bunch spacing was made in July.

Table 2: Overview of LHC Machine and Beam Parameters for Run 2 Compared to the Design Values

| Parameter | Beam type: | Design | 2015 | 2016 | 2017 | | 2018 | |
|--|------------|--------|------|-----------|------|----------------------|-------------------------|-------------------------|
| | | Std | Std | Std/BCMS | BCMS | 8b4e | 8b4e-BCS | BCMS |
| Energy [TeV] | | 7 | 6.5 | 6.5 | 6.5 | 6.5 | 6.5 | 6.5 |
| Number of bunches per ring | | 2808 | 2244 | 2040/2076 | 2556 | 1916 | 1868 | 2556 |
| Bunch spacing [ns] | | 25 | 25 | 25 | 25 | 25 | 25 | 25 |
| Bunch population N_b [10^{11} p/b] | | 1.15 | 1.15 | 1.2 | 1.2 | 1.2 | 1.25 | 1.1 |
| Transv. norm. emittance ⁽⁴⁾ ϵ_n [mm-mrad] | | 3.75 | 3.5 | 3.5/2.1 | 2.1 | 2.3 | 1.8 | 2 |
| Betatron function at IP1 and IP5 β^* [m] | | 0.55 | 0.8 | 0.4 | 0.4 | 0.4/0.3 | 0.3 | 0.3/0.25 ⁽¹⁾ |
| Half crossing angle [μ rad] | | 142.5 | 145 | 185/140 | 150 | 150 | 150/120 ⁽²⁾ | 160/130 ⁽²⁾ |
| Peak luminosity [10^{34} cm ⁻² s ⁻¹] | | 1 | 0.55 | 0.83/1.4 | 1.74 | 1.9 | 2.06/1.5 ⁽³⁾ | 2.1 |
| Maximum pile up μ (per bunch crossing) | | ~20 | ~15 | ~20/35 | ~45 | 70/60 ⁽²⁾ | 80/60 ⁽³⁾ | 60 |
| Stored beam energy [MJ] | | 360 | 270 | 345 | 320 | 240 | 245 | 320 |
| Number days of physics operation | | n.a. | 88 | 146 | | 140 | | 145 |
| Integrated luminosity per year [fb ⁻¹] | | n.a. | 4.2 | 39.7 | | 50.6 | | 66 |

⁽¹⁾ Minimum betatron function during betatron anti-levelling

⁽³⁾ Value after luminosity-levelling by separation

⁽²⁾ Minimum crossing angle during crossing angle anti-levelling

⁽⁴⁾ Value at maximum energy in stable beams

The β^* at the interaction points IP1 (ATLAS) and IP5 (CMS) was set at 80 cm, well above the design value of 55 cm to ensure an aperture safety margin [11-13]. The β^* at IP2 (ALICE) was set at 10 m and IP8 (LHCb) at 3 m. The length of the injected bunch trains was limited to 144 bunches per injection as a result of the lower-than-expected damage limit of the Boron Nitrite injection absorbers blocks [14], resulting in a total of 2244 bunches per beam. The tune and chromaticity feedforward corrections at injection and the first part of the energy ramp, to compensate for the magnetic multipole drifts resulting from the redistribution of the current in the superconducting cables, was successfully consolidated for 6.5 TeV operation [15, 16].

The 2016 run started with the standard 25 ns bunch spacing and β^* for IP1 and IP5 was reduced to 40 cm, which allowed reaching the design peak luminosity value of 1×10^{34} cm⁻²s⁻¹ in June. A vacuum leak on the SPS beam dump limited the bunch-train length at injection also for 2016 to 144 bunches per injection. Nevertheless, in July the high-brightness beam, based on Bunch Compressions, Merging and Splitting (BCMS) became operationally available from the injectors with initially with 96 bunches per injection, but later also with 144 bunches per injection [17]. For the same bunch intensity, the transverse emittance was reduced from ~3.5 mm-mrad to ~2.1 mm-mrad. This together with a reduction of the crossing angle from 370 μ rad to 280 μ rad and the β^* of 40 cm resulted in a record peak luminosity in 2016 of 1.4×10^{34} cm⁻²s⁻¹.

The 2017 run, started with the BCMS beam and a β^* of 40 cm [18]. However, during the beam vacuum pump down, following the replacement of a dipole magnet during the winter stop, about 7 liters of air entered accidentally in the beam vacuum and froze locally on the cold surface of the interconnection of cell 16L2. This caused abnormal background radiation and sudden beam losses, some leading to beam dumps [19, 20]. Attempts to evaporate the frozen gas from the beam screen and condensate

it on the cold bore were unsuccessful. The heat load as a result of e-cloud production enhanced the loss mechanism. Therefore, alternative beam production schemes, reducing considerably the heat load, were setup in the injector chain, providing bunch trains of 8 bunches and 4 empty buckets (8b4e and later 8b4e-BCS). This beam, which has an even higher brightness than the BCMS one, produced an even higher pile-up level in the experiments and luminosity levelling down to 1.5×10^{34} cm⁻²s⁻¹ was required for ATLAS and CMS. Aperture measurements revealed an additional margin that was sufficient to decrease the β^* in IP1 and IP5 to 30 cm, resulting in a new peak luminosity record of 2.06×10^{34} cm⁻²s⁻¹.

Despite the 16L2 issue, the year was completed successfully and the integrated luminosity of 50.6 fb⁻¹ was 10% higher than initially foreseen.

For the 2018, run the 16L2 issue was in part solved by a partial warming up to 90 K. The gasses were pumped, but the water vapor remained, still causing an increased background radiation, but only very few beam dumps, while running the BCMS beam at $\sim 1.1 \times 10^{11}$ protons per bunch and 2556 bunches per beam. The 2018 machine configuration was very much a continuation of 2017. The various levelling schemes were further developed and used operationally in anti-levelling mode to further optimize luminosity production [21]. The integrated luminosity of 66 fb⁻¹ surpassed the initial estimate by 10%.

MAIN REMAINING OPERATIONAL CHALLENGES

Electron Cloud and Cryogenic Heat Load

Electron cloud has been observed in the LHC since bunch trains were used, and represents one of the main performance limitations for the LHC [22, 23]. It causes transverse emittance blow up and potentially run the beam unstable, causing beam losses. In addition, e-cloud production puts a large constraint on the cryogenic system

Content from this work may be used under the terms of the CC BY 3.0 licence (© 2019). Any distribution of this work must maintain attribution to the author(s), title of the work, publisher, and DOI

as it represents the major source of heat load to the beam screen. The production of e-cloud strongly depends on the secondary electron emission yield (SEY) of the beam screen. Simulations and experience have shown that e-cloud can be mitigated to a large extent by exposing the surface of the beam screen for prolonged periods of time to high rates of e-cloud (the so-called scrubbing) [24]. However, observations in the second half of Run 2 revealed that not all eight ring sectors behave similarly and a significant spread in heat load between the sectors remained constant, unlike Run 1, where this spread was not present [25].

In practice, at the start of a yearly run and once the LHC is sufficiently commissioned to be filled with a large number of bunches at low energy, a scrubbing run is scheduled to reestablish conditions that allow accelerating safely a substantial number of bunches to high energy for collisions. The running for physics will then further, although more slowly, scrub the machine. For the high heat load and its large spread, a task force has been put in place to gather and study all the information related to the heat load spread and to identify the source of the unexpected high SEY and to define a mitigation strategy.

Transverse Emittance Growth

Together with the beam intensity the transverse emittance is one of the main parameters for high luminosity production, to be preserved by minimizing blow up in any of the stages of the LHC cycle. Measurement campaigns have revealed that the transverse emittance increases more than estimated by simulations, principally during the injection plateau and acceleration [26, 27]. The main contribution to the transverse emittance growth appears during acceleration. Up to $\sim 45\%$ in the vertical plane for the highest brightness beam (8b4e-BCS) and $\sim 22\%$ for the BCMS beam have been observed (Table 3). Minimizing this growth will directly translate in a higher peak luminosity. However, the mechanism behind the blow up is not yet fully understood and a working group, combining all the observations and concentrating efforts to understand and possibly mitigate the issue has been established [28]. Minimizing this emittance growth will be very important, as during Run 3 the beam brightness from the upgraded injectors will further increase [29].

Table 3: Measured Transverse Emittance Growth Per Process and Beam Type

| Process | BCMS | | 8b4e-BCS | |
|--------------|-------|-------|----------|-------|
| | H [%] | V [%] | H [%] | V [%] |
| Injection | 15 | 9 | 17 | 15 |
| Acceleration | 5 | 22 | 43 | 45 |

PREPARING FOR THE HL-LHC

Some methods and principles necessary for the operation of the HL-LHC [30] have already been implemented and tested in the LHC with the aim to validate them and to gain valuable operational experience at an early stage.

Achromatic Telescopic Squeeze Optics

The Achromatic Telescopic Squeeze (ATS) Optics allows for very small β^* values in the IPs, while correcting the chromatic aberrations induced by the inner triplets on either side of the experiments, required for the HL-LHC [31]. The ATS Optics is based on a two-stage telescopic squeeze, initially using as usual the matching quadrupoles around IP1 and IP5 and in a second stage by acting on the insertion devices of the neighboring Interaction Regions, IR2 and IR8 for IP1 and IR4 and IR6 for IP5. The LHC was designed for a β^* at IP1 and IP5 of 55 cm (Table 2), while the HL-LHC foresees to go as low as 15 cm.

The ATS scheme was tested and validated during dedicated machine development (MD) sessions and came to sufficient maturity in 2016 to be deployed operationally in 2017 [32]. The β^* was initially squeezed down to 40 cm, using the ATS pre-squeeze and a further step down to 30 cm, using the telescopic effect, was made successfully in the second half of the 2017. In 2018, as part of the anti-levelling scheme, the β^* was further reduced to 25 cm.

Luminosity Levelling and Anti-Levelling

Luminosity levelling is generally applied to reduce the number of collisions per bunch crossing in the experiments when the instantaneous luminosity is too high. This levelling has been done routinely for the two low luminosity experiments in IP2 and IP8 [33]. However, in 2017, when the 8b4e and the 8b4e-BCS beams were used the peak luminosity exceeded the pile up limit of ATLAS and CMS, hence levelling by beam separation was applied too. Levelling by changing the crossing angle was deployed in 2017 and in 2018 the levelling by β^* was added. Since in 2018 there was no need for levelling, they were both actually used in anti-levelling mode. After sufficient luminosity burn-off during collisions, the dynamic aperture increases allowing for the anti-levelling through a reduction of the crossing angle from 300 μrad to 240 μrad and later also the β^* from 30 cm to 25 cm, resulting in a small increase of the instantaneous luminosity, but more importantly in the operational experience with these schemes.

CONCLUSIONS

LHC Run 2 has been completed successfully and has produced 160 fb^{-1} of integrated luminosity for ATLAS and CMS. The machine and beam performance have continuously improved, but there are still challenges among which heat load spread and emittance growth.

Run 2 also saw important steps towards HL-LHC operation with the deployment of the ATS optics and various schemes of luminosity levelling and anti-levelling.

ACKNOWLEDGEMENTS

The authors thank all the persons and teams that made a big effort to reach these outstanding machine and beam performances during Run 2 and are in debt to many of them for the material used for this publication.

REFERENCES

- [1] J. Wenninger, “Operation and Configuration of the LHC in Run 2”, CERN, Geneva, Switzerland, CERN-ACC-NOTE-2019-0007.
- [2] J. M. Jowett *et al.*, “The 2015 Heavy-Ion Run of the LHC”, *7th Int. Particle Accelerator Conf. (IPAC'16)*, Busan, Korea, May 2016, pp. 1493-1496. TUPMW027.
- [3] J. M. Jowett *et al.*, “The 2016 Proton-Nucleus Run of the LHC”, in *Proc. 8th Int. Particle Accelerator Conf. (IPAC'17)*, Copenhagen, Denmark, May 2017, pp. 2071-2074. doi:10.18429/JACoW-IPAC2017-TUPVA014
- [4] R. Alemany-Fernandez *et al.*, “Performance of the CERN Injector Complex and Transmission Studies into the LHC during the Second Proton-Lead Run”, *8th Int. Particle Accelerator Conf. (IPAC'17)*, Copenhagen, Denmark, May 2017, pp. 2395-2398. TUPVA128
- [5] M. Schaumann *et al.*, “First Xenon-Xenon Collisions in the LHC”, *9th Int. Particle Accelerator Conf. (IPAC'18)*, Vancouver, Canada, Apr.-May 2018, pp. 180-183. MOPMF039
- [6] J. M. Jowett *et al.*, “The 2018 Heavy-Ion Run of the LHC”, *10th Int. Particle Accelerator Conf. (IPAC'19)*, Melbourne, Australia, May 2019, paper WEYYPLM2, this conference.
- [7] B. Todd *et al.*, “LHC Availability 2016: Proton Run”, CERN, Geneva, Switzerland, CERN-ACC-Note-2016-0067.
- [8] B. Todd *et al.*, “LHC Availability 2017: Proton Run”, CERN, Geneva, Switzerland, CERN-ACC-Note-2017-0063.
- [9] B. Todd *et al.*, “LHC Availability 2018: Proton Run”, CERN, Geneva, Switzerland, CERN-ACC-Note-2018-00681.
- [10] O. Brüning, P. Collier, P. Lebrun, S. Myers, R. Ostojic, J. Poole, P. Proudlock (Eds). “LHC Design Report Vol. 1”, CERN, Geneva, Switzerland, CERN-2004-003-V-1.
- [11] R. Bruce, S. Redaelli, “Collimation and β^* Reach”, *5th Evian Workshop on LHC Beam Operation*, Evian, France, CERN-ACC-2014-0319.
- [12] G. Papotti *et al.*, “LHC Operation at 6.5 TeV: Status and Beam Physics Issues”, *North American Particle Accelerator Conf. (NAPAC'16)*, Chicago, IL, USA, Oct. 2016, pp. 37-41. MOB3IO02.
- [13] G. Papotti *et al.*, “Operation of the LHC with Protons at High Luminosity and High Energy”, *7th Int. Particle Accelerator Conf. (IPAC'16)*, Busan, Korea, May 2016, pp. 2066-2069. WEOCA01.
- [14] A. Lechner, “TDI”, *6th Evian Workshop on LHC Beam Operation*, Evian, France, CERN-ACC-2015-376.
- [15] M. Solfaroli Camillocci, *et al.*, “Feed-Forward Corrections for Tune and Chromaticity Injection Decay During 2015 LHC Operation”, *7th Int. Particle Accelerator Conf. (IPAC'16)*, Busan, Korea, May 2016, pp. 1489-1492. TUPMW026.
- [16] M. Schaumann, *et al.*, “Tune and Chromaticity Control During Snapback and Ramp in 2015 LHC Operation”, *7th Int. Particle Accelerator Conf. (IPAC'16)*, Busan, Korea, May 2016, pp. 1501-1504. TUPMW029.
- [17] H. Damerou, *et al.*, “RF Manipulations for Higher Brightness LHC-type Beams”, *4th Int. Particle Accelerator Conf. (IPAC'13)*, Shanghai, China, May 2013, pp. 2600-2602. WEPEA044
- [18] B. Salvachua *et al.*, “LHC Operational Scenarios During 2017 Run”, *9th Int. Particle Accelerator Conf. (IPAC'18)*, Vancouver, Canada, Apr.-May 2018, pp. 220-223. MOPMF051.
- [19] J. M. Jimenez *et al.*, “Observations, Analysis and Mitigation of Recurrent LHC Beam Dumps Caused by Fast Losses in Arc Half-Cell 16L2”, *9th Int. Particle Accelerator Conf. (IPAC'18)*, Vancouver, Canada, Apr.-May 2018, pp. 228-231. MOPMF053.
- [20] B. Salvant *et al.*, “Experimental Characterisation of a Fast Instability Linked to Losses in the 16L2 Cryogenic Half-Cell in the CERN LHC”, *9th Int. Particle Accelerator Conf. (IPAC'18)*, Vancouver, Canada, Apr.-May 2018, pp. 3103-3106. THPAF058.
- [21] N. Karastathis, *et al.*, “Crossing Angle Anti-Leveling at the LHC in 2017”, *9th Int. Particle Accelerator Conf. (IPAC'18)*, Vancouver, Canada, Apr.-May 2018, pp. 184-187. MOPMF040.
- [22] G. Iadarola *et al.*, “Electron Cloud and Scrubbing Studies for the LHC”, *4th Int. Particle Accelerator Conf. (IPAC'13)*, Shanghai, China, May 2013, pp. 1331-1333. TUPFI002.
- [23] G. Rumolo *et al.*, “Electron Cloud Effects at the LHC and LHC Injectors”, *8th Int. Particle Accelerator Conf. (IPAC'17)*, Copenhagen, Denmark, May 2017, pp. 30-36. MOZA1.
- [24] G.H. I. Maury Cuna, *et al.*, “Simulation of electron-cloud heat load for the cold arcs of the large hadron collider”, *3rd Int. Particle Accelerator Conf. (IPAC'12)*, New Orleans, LA, USA, May 2012, pp. 115-117. MOPPC001,
- [25] G. Skripka, *et al.*, “Comparison of Electron Cloud Build-Up Simulations Against Heat Load Measurements for the LHC Arcs with Different Beam Configurations”, *10th Int. Particle Accelerator Conf. (IPAC'19)*, Melbourne, Australia, May 2019, WEPTS051, this conference.
- [26] M. Hostettler *et al.*, “Comparison of Transverse Emittance Measurements in the LHC”, *8th Int. Particle Accelerator Conf. (IPAC'17)*, Copenhagen, Denmark, May 2017, pp. 377-380. MOPAB110.
- [27] S. Papadopoulou *et al.*, “Monitoring and Modelling of the LHC Emittance and Luminosity Evolution in 2018”, *10th Int. Particle Accelerator Conf. (IPAC'19)*, Melbourne, Australia, May 2019, WEPTS046, this conference.
- [28] LHC Emittance Preservation Working Group, <https://indico.cern.ch/category/10421/>
- [29] J. Coupard *et al.* (Eds), “LHC Injectors Upgrade Technical Design Report – Volume 1: Protons”, CERN, Geneva, Switzerland, CERN-ACC-2014-0337.
- [30] G. Apollinari, *et al.*, (Eds) “High-Luminosity Large Hadron Collider (HL-LHC) Technical Design Report Vol. 0.1”, CERN, Geneva, Switzerland, CERN-2017-007-M.
- [31] S.D. Fartoukh *et al.*, “The Achromatic Telescopic Squeezing Scheme: Basic Principles and First Demonstration at the LHC”, *3rd Int. Particle Accelerator Conf. (IPAC'12)*, New Orleans, LA, USA, May 2012, pp. 1978-1980. TUPPR068.
- [32] M. Pojer *et al.*, “LHC Operational Experience of the 6.5 TeV Proton Run with ATS Optics”, *9th Int. Particle Accelerator Conf. (IPAC'18)*, Vancouver, Canada, Apr.-May 2018, pp. 216-219. MOPMF050.
- [33] M. Hostettler *et al.*, “LHC Luminosity Performance”, CERN, Geneva, Switzerland, CERN-THESIS-2018-051.